

The SIEGFRIED system was developed in this laboratory for mass identification in association with our general studies of nuclei far from beta stability. Simplistically, this system accelerates He-jet deposited beta decay recoils from a collecting plate across a constant potential (6-12kV) to a CEMA detector. An initial start signal is obtained in a plastic scintillator from a  $\beta$ - or  $\gamma$ -ray associated with the decay and the time of flight is recorded with a time to pulse height converter. A typical recoil spectrum produced by 70 MeV  $^3\text{He}$  on  $^{27}\text{Al}$  is shown in Fig. 1. Although the intrinsic electronic timing in this experiment is  $\leq 1$  nsec FWHM, the mass peak widths are of order 100 nsec. This broadening has been interpreted as resulting from the inherent recoil energy which is here 300-400 eV. Initial recoil energies are a substantial fraction of the final total kinetic energy. It is the intention of this study to unfold the recoil energy distribution and obtain decay energies and Fermi to Gamow-Teller mixing ratios.

The normal distribution of recoil energies for Fermi and Gamow-Teller transitions is shown in Fig. 2. Comparison of these distributions with experiment shows severe problems caused by the large angle of acceptance as well as source thickness in SIEGFRIED. In addition, coincident  $\gamma$ -rays further confuse matters as indicated by the  $^{28}\text{Al}$  peak in Fig. 1 which is significantly broadened with respect to the other peaks, all of which contain far less  $\gamma$ -ray intensity. Nevertheless, it is hoped that the mass spectra may be parametrized using known transitions to analyze new peaks of interest. To test this hypothesis, we have analyzed the  $^{23}\text{Mg}$ ,  $^{25}\text{Al}$ , and  $^{27}\text{Si}$  mass recoil peaks in Fig. 1 because they are essentially pure ground state mirror transitions which are well known. A similar mass spectrum produced by 42 MeV  $^4\text{He}$  on  $^{27}\text{Al}$  +  $^{20}\text{Ne}$  was also analyzed using the  $^{18}\text{F}$ ,  $^{27}\text{Si}$ , and  $^{29}\text{P}$  mass peaks. The natural parametrization for the recoil width is given from classical physics as

$$\Delta E_R = aA \left(\frac{\Delta t}{t}\right) [(1-f) + bf] + c$$

where  $\Delta t$  is the width of the peak,  $t$  is the mean time of flight, and  $f$  is the fraction of Gamow-Teller decay for mass A. Parameters  $a$  and  $c$  are to be fixed by experiment and contain energy cut-offs and other systematic irregularities. The  $b$  parameter represents the ratio of pure Fermi to pure Gamow-Teller widths and will be fixed by theory. In this discussion  $\Delta T$  is the full width at half maximum as generated by the fitting routine SAMPO and  $b=0.483$ . Thus, for each data set we have a two parameter fit to three points.

The results of this fitting procedure are summarized in Table I. The data can be fitted in

two ways, first supplying the fraction F/GT and fitting to the energies and second reversing that procedure. We also fit the data for the first case by ignoring F-GT information. This fit was rather poor, yielding a  $\chi^2=9$ . Replacing the F-GT information from theory, we get excellent fits with  $\chi^2=0.07$  in the first case and  $\chi^2=0.05$  in the second case. These results are embarrassingly good and suggest that this procedure may be quite profitable. Nevertheless, the paucity of data makes any conclusions premature. In the near future we intend to obtain a larger data set in a single experiment in order to more accurately test these techniques.

Table I. Mass TOF fitted data

Decay	Literature	$\Delta E_R$ (eV)		% GT	
		TOF <sup>2</sup>	TOF + F/GT Theory	Theory	Fitted
<b>Case 1:</b>					
$^{23}\text{Mg} \rightarrow ^{23}\text{Na}$	281.7	283(8)	283(8)	29.2	29.3
$^{25}\text{Al} \rightarrow ^{25}\text{Mg}$	299.4	343(20)	297(19)	42.4	42.1
$^{27}\text{Si} \rightarrow ^{27}\text{Al}$	362.4	335(13)	364(10)	34.1	34.2
<b>Case 2:</b>					
$^{18}\text{F} \rightarrow ^{18}\text{O}$	31.3	--	31(9)	100	100
$^{27}\text{Si} \rightarrow ^{27}\text{Al}$	362.4	--	369(32)	34.1	36.2
$^{29}\text{P} \rightarrow ^{29}\text{Si}$	357.4	--	356(15)	20.6	20.1

1. Corrected for 9% decay to excited states.
2. Fitted ignoring F/GT information.

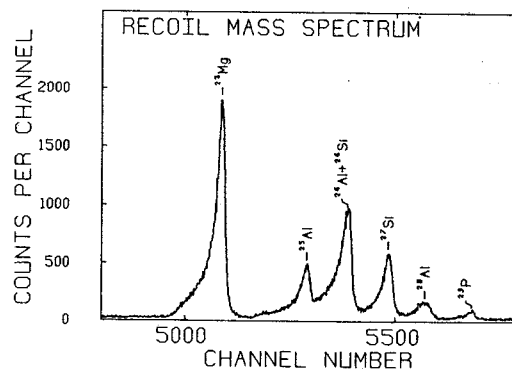


Fig. 1

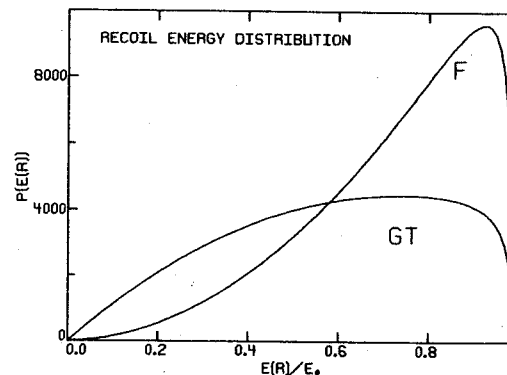


Fig. 2

It is well known from the shell model and experiment that the magic number of 50 protons or neutrons is a particularly stable configuration. It would be interesting, therefore to produce the doubly magic nucleus  $^{100}\text{Sn}$ . Currently,  $^{106}\text{Sn}$  is the lightest tin to have been positively identified. We have performed ALICE<sup>1</sup> reaction cross section calculations which show fairly high cross sections for making  $^{104-106}\text{Sn}$  with up to 76 MeV  $^3\text{He}$  beams from the Michigan State University 50 MeV cyclotron using a  $^{106}\text{Cd}$  target. The maximum calculated cross sections are shown in Table I for isotopes of interest. With the new 500 MeV heavy ion cyclotron, production of  $^{100}\text{Sn}$  should be possible.

Recently, we began to record excitation functions with 65-75 MeV  $\tau$  beams onto a target of CdO enriched to approximately 90%  $^{106}\text{Cd}$  and supported by a 0.05 mm Al foil backing. We counted the activities produced with Ge(Li) detectors situated out of beam in a low background counting

area. Transport was achieved by a Helium Jet Recoil Transport System.<sup>2</sup> Half-lives as low as 0.1 seconds can be determined by this method.

A series of four consecutive 30 s spectra were taken using the data acquisition program HYDRA.<sup>3</sup> Another computer code POLYBAND<sup>4</sup> was used to determine half-lives. These results are shown in Table II. Many  $\gamma$ 's either decayed away too quickly to be measured in this experiment or were long-lived. Also, the stronger  $\gamma$ -rays in these spectra were identified by comparison with the literature. Table III identifies some of the stronger-observed  $\gamma$ 's and their tentative assignments. Completion of the excitation function at lower energies, and other experiments such as more  $t_{1/2}$ ,  $\gamma$ - $\gamma$ , x- $\gamma$ ,  $\gamma$ -mass coincidence are planned to help identify the new isotopes.

1. M. Blann and F. Plasil, ALICE: A Nuclear Evaporation Code, U.S. Atomic Energy Commission Report No. COO-3494-10, 1973
2. K.L. Kosanke, M.S. Edmiston, R.A. Warner, R.B. Firestone, and Wm. C. McHarris, Nucl. Instr. Meth. 17 (1965) 78
3. R. Au, HYDRA, Michigan State University Cyclotron Laboratory Sigma-7 Program Description Book
4. S. Faber, POLYBAND: A Least Squares Routine, unpublished.

Table II Maximum Calculated Cross Sections for  $^{106}\text{Cd}(^3\text{He}, xn+yp+z\alpha)$  Reaction Products

Nuclide	Calculated Cross Section(mb)	$^3\text{He}$ Beam Energy (MeV)
$^{106}\text{Sn}$	450	30
$^{105}\text{Sn}$	37	50
$^{104}\text{Sn}$	32	63
$^{106}\text{In}$	68	34
$^{105}\text{In}$	330	40
$^{104}\text{In}$	24	58
$^{103}\text{In}$	24	75
$^{106}\text{Cd}$	415	30
$^{105}\text{Cd}$	350	45
$^{104}\text{Cd}$	530	60
$^{103}\text{Cd}$	370	36
$^{102}\text{Cd}$	520	47
$^{101}\text{Cd}$	115	65
$^{104}\text{Ag}$	14	65
$^{103}\text{Ag}$	150	33
$^{102}\text{Ag}$	78	52
$^{101}\text{Ag}$	370	60
$^{102}\text{Pd}$	135	50
$^{101}\text{Pd}$	150	65
$^{100}\text{Pd}$	440	76
$^{99}\text{Pd}$	130	53
$^{98}\text{Pd}$	280	67
$^{97}\text{Pd}$		

Table II. Experimental Half-Lives

$E_\gamma$ (keV)	$t_{1/2}$ (min)	Tentative Assignment
131.2	5.79±0.55	$^{105}\text{In}$
260.9	7.77±0.36	$^{105}\text{In}$
658.0	1.86±0.26	$^{104}\text{In}$
833.7	1.90±0.05	$^{104}\text{In}$
877.4	1.66±0.18	?
942.4	1.97±0.19	?
998.3	4.06±0.52	$^{106}\text{In}$

Table III. Identified Products for 70 MeV  $^3\text{He}$  on  $^{106}\text{Cd}$

Reaction Product	Strongest $\gamma$ -rays (keV)
$^{106}\text{In}$	632.7, 860.7
$^{105}\text{In}$	131.2, 260.9, 604.3
$^{105}\text{Cd}$	1301.4, 1693.6
$^{104}\text{Cd}$	709.3
$^{102}\text{Cd}$	480.9
$^{105}\text{Ag}$	280.8
$^{104}\text{Ag}$	556.3, 767.5, 942.4
$^{103}\text{Ag}$	118.3, 148.1, 243.8
$^{101}\text{Pd}$	296.6
$^{100}\text{Pd}$	73.4

High Spin States in  $^{116}\text{Sb}$   
W. H. Bentley and W.H. Kelly

Nuclei near closed shells are of interest because of the relative simplicity their level structure should display. The Sb nuclei with one proton outside the closed  $Z=50$  shell are examples of such nuclei. As a continuation of the ongoing study of Sb nuclei, experiments were performed to excite the high spin states in  $^{116}\text{Sb}$ . The reaction used in this study was the  $(\alpha, 3n\gamma)$  reaction. The experiments performed included  $\gamma$ - $\gamma$  coincidence,  $\gamma$  angular distributions and  $\gamma$  half life measurements. The target used was a natural Indium foil.

The coincidence experiment was performed using a 38 MeV alpha beam provided by the M.S.U. Cyclotron. Two high resolution Ge(Li) detectors were positioned near the target each at right angles with respect to the beam direction. The energy information from each detector, along with a parameter giving the time between detection of the two  $\gamma$ -rays, were event recorded on magnetic tape. About thirty million events were collected. These were then sorted into background subtracted coincidence spectra.

The gamma ray angular distribution measurements were performed with a Ge(Li) detector mounted on the arm of the M.S.U. goniometer apparatus. Singles  $\gamma$ -ray spectra were taken at various random angles measured with respect to the beam direction. Intensity normalization between angles was determined by counting elastically scattered alphas with a Si surface barrier detector kept at a fixed angle. Individual peak intensities were extracted and fitted to an expansion of Legendre Polynomials. The resulting  $A_2$  and  $A_4$  coefficients were then compared with theoretical values to determine probable transition multipolarities.

The  $\gamma$ -ray half life experiment was performed using the M.S.U. beam sweeper which allows only regularly selected cyclotron beam bursts through to the target. A timing signal with respect to the last occurring beam burst is then given to the computer in coincidence with each Ge(Li) energy signal. A computer program then divides the energy signals into ten time bands.  $\gamma$ -ray intensities from each band are later extracted and fitted to a half life curve.

From the coincidence spectra and intensity information a level scheme was determined. This is shown in Fig. 1. All of the levels shown decay through the  $J=8^-$  isomer. Therefore the absolute excitation energies of these levels are not accurately known, but depend on the energy of this isomer. An approximate determination of  $225 \pm 60$  KeV has been made by R. Kamermans et al <sup>1)</sup> for this level. This is the value which is used in Fig. 1. Also note the spin assignments for all of the levels are based on

the known  $8^-$  spin of this isomeric level. <sup>2)</sup>

A comparison of the  $^{116}\text{Sb}$  level scheme shown here with that of  $^{118}\text{Sb}$  given in a previous annual report <sup>3)</sup> immediately demonstrates the similarity in the high spin structure of these two nuclei. The two bands reported in  $^{118}\text{Sb}$  also appear in  $^{116}\text{Sb}$ . The higher lying band was excited up to the fifth band member. Unfortunately the angular distribution results were inconclusive in determining the spin of the level this band is built on. Values for this spin of  $J=7$  and  $J=9$  are both consistent with the data. A plot of  $\Delta E$  vs  $2I^2$  is shown in Fig. 2. The band is plotted  $^{2I}$  in this figure for each of the two possible spin values. It is compared with the corresponding band in  $^{118}\text{Sb}$ . The similarity in the two bands is immediately evident. Also evident is the accuracy to which these bands fit the  $\frac{h^2}{2\theta} I(I+1)$  energy spacing of a normal rotational band. Such a band would appear as a horizontal line on this type of plot. This is clear evidence of relatively low lying deformed states in odd-odd Sb nuclei.

The second band which is built on a proposed  $J=7$  state is populated only very weakly in  $^{116}\text{Sb}$ . Evidence for the existence of the first two members of this band is found in the coincidence data. However, because the energies of these transitions are so close to that of much stronger transitions in the spectrum, it is difficult to obtain much accurate information about them. It is clear that they do not follow the simple rotational energy sequence as well as the higher lying band does. They do, however, appear to follow a pattern like that of the corresponding band in  $^{118}\text{Sb}$ , which was populated rather strongly. These bands are also shown in Fig. 2.

The existence of such bands in the odd-odd Sb nuclei is not unexpected. Experiments by Gaigales et al <sup>4)</sup> studying the high spin states of odd mass Sb nuclei have shown that bands built on a  $9/2^+$  state occur from  $A=113$  to  $A=119$ . These bands have generally been described as rotational bands built on a deformed  $g^{9/2}$  proton hole state. It is therefore reasonable to expect similar band structures might occur in the odd-odd nuclei based on the same proton state coupled to various neutron states. Evidence supporting such an assignment to the observed odd-odd bands can be given. First, the excitation energy of the proposed  $J=7$  band is very nearly the same as that of the  $9/2^+$  band in the adjacent odd mass Sb nuclei. In addition the high spin of the odd-odd bands would require a relatively high spin contribution from the proton particle state. The  $g^{9/2}$  hole state is the only easily available high spin state for the proton. Finally, the similar-

ities in the intraband transition energies as a function of angular momentum, between the odd-odd and odd mass bands, would tend to indicate similar internal structure. This can also be seen in Fig. 2.

In conclusion the high spin structure of  $^{116}\text{Sb}$  is very similar to that of  $^{118}\text{Sb}$ , with both nuclei displaying definite rotational behavior. It is also apparent that this rotational structure is closely related to the known  $9/2^+$  bands in the adjacent odd mass Sb nuclei.

1. R. Kamermans, H.W. Jongsma, T.J. Ketel, R. Van Der Wey and H. Verheul, Nuclear Physics A226 (1976) 346
2. C. Ekstrom, W. Hogervorst, S. Ingelman and G. Wannberg, Nuclear Physics A226 (1974) 219
3. W.H. Bentley, C.B. Morgan, R.A. Warner, W.H. Kelly, R. Shamu and E.M. Bernstein, Annual Report 1976-77 Cyclotron Laboratory Michigan State University 40
4. A.K. Gaigalas, R.E. Shroy, G. Schatz, and D.B. Fossan, Physical Review Letters 35 (1975) 555

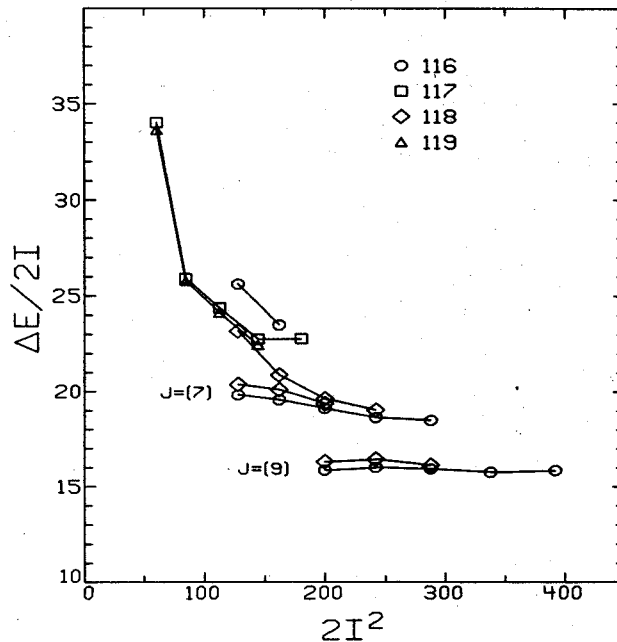


Fig. 2. The rotational band spacing as a function of  $I^2$  for the bands in Sb.

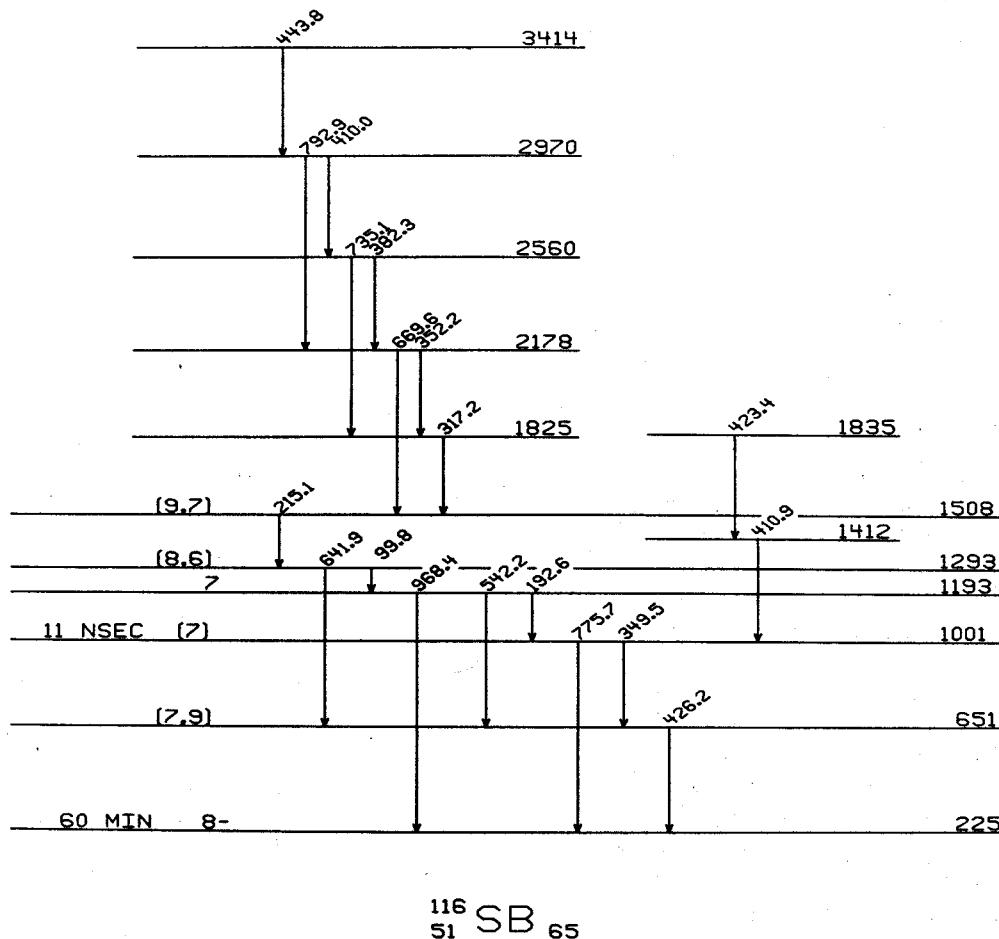


Fig. 1. Partial level scheme for  $^{116}\text{Sb}$  showing those states populated in the  $^{115}\text{In}(\alpha, 3n\gamma)$  reaction.

Considerable effort has been expended at the MSU Cyclotron Laboratory in the study of the neutron deficient Gd isotopes produced by the  $^{144}\text{Sm} (^3\text{He}, \text{xn})$  reaction. Elaborate decay scheme work has been performed for  $^{145}\text{Gd}^{g+m}$  <sup>1</sup> which has contributed important insights into beta decay. More recently we have published the  $^{143}\text{Gd}^{g+m}$  <sup>2</sup> decay schemes which show a marked difference from the systematics of  $^{145}\text{Gd}$  decay apparently associated with the departure from the  $N=82$  closed shell. With the available 76 MeV  $^3\text{He}$  beam from the MSU Cyclotron it is possible to produce the new isotope  $^{141}\text{Gd}$ . To test the feasibility for  $^{141}\text{Gd}$  production, we have performed cross section calculations with the particle evaporation code ALICE. <sup>3</sup> This code has proven qualitatively descriptive for predicting the relative  $^{143-145}\text{Gd}$  productions. The results of this calculation are shown in Fig. 1. At 76 MeV  $^3\text{He}$  the  $^{141}\text{Gd}$  cross section is calculated to be at its peak of 26 mb. This represents 1.2% of the total calculated compound nucleus cross section. Clearly, a formidable problem may exist in identifying  $^{141}\text{Gd}$  from the background.

In order to search for  $^{141}\text{Gd}$  it is helpful to utilize the systematics of the lighter odd-A,  $N=77$  nuclei. These are all characterized by an  $11/2^- \rightarrow 5/2^+$  E3 isomeric decay with little or no  $\beta$ -decay competition. The single particle matrix element for this E3 decay is observed to decrease significantly with increasing  $Z$  while the E3  $\gamma$ -ray decay energy peaks at  $^{137}\text{Nd}$  and falls rapidly at  $^{139}\text{Sm}$ . Following these systematics, the  $^{141}\text{Gd}$  E3 should have a half-life greater than 1 min., and it is likely that this isomer will either  $\beta$  decay and/or proceed by an M4 transition through the  $3/2^+$  state. The ground state of  $^{141}\text{Gd}$  is expected to be  $1/2^+$  and the half-life of the lighter  $N=77$  ground state decays is seen to plummet from 17h for  $^{135}\text{Ce}$  to 2.5 min. for  $^{139}\text{Sm}$ . The half-life for  $^{141}\text{Gd}$  decay then extrapolates to about 30s. Unfortunately, it is likely that the  $^{141}\text{Gd}$  decay will proceed to numerous excited states in  $^{141}\text{Eu}$  and it is possible that no single  $\gamma$ -ray transition will be easily observable.  $^{141}\text{Gd}$   $\beta$ -decay should occur with a longer  $t_{1/2}$  than the ground state decay, and it will feed numerous levels in  $^{141}\text{Eu}$  which all deexcite through the first excited  $11/2^-$  state. This state has been observed as a 3.3s isomer in  $^{141}\text{Eu}$  <sup>4</sup> deexciting to the ground state via a 96 keV E3  $\gamma$ -ray transition. The key to detecting  $^{141}\text{Gd}$  decay is therefore to look for a 96 keV transition appearing with a half-life longer than 3.3s.

A series of excitation functions for 30-76 MeV  $^3\text{He}$  on  $^{144}\text{Sm}$  has been performed in approximately 6 MeV steps. Numerous  $\gamma$ -rays were observed corresponding to known activities and after extensive analysis all but 5-6  $\gamma$ -rays were placed either

in known decay schemes or eliminated from consideration as  $^{141}\text{Gd}$  decay because of their appearance in the 60 MeV spectrum where insufficient energy is present for  $^{141}\text{Gd}$  production. Among those remaining  $\gamma$ -rays is the 96 keV  $\gamma$ -ray attributed to  $^{141}\text{Eu}$ . A half-life measurement was performed on this  $\gamma$ -ray where six 45s consecutive spectra were taken with an internal pulser for deadtime correction. A  $4.5 \pm 0.9$  min. half-life was observed and the half-life plot we obtained is shown in Fig. 2. While this is still only weak evidence for the existence of  $^{141}\text{Gd}$ , no other 96-keV transition is known in this region. Further experiments, including x- $\gamma$  coincidence and an improved half-life measurement, are planned to find other  $^{141}\text{Gd}$  transitions.

1. R.E. Eppley, Wm. C. McHarris, and W.H. Kelly, Phys. Rev. (3) (1971) 282. A more complete study of  $^{145}\text{Gd}$  is about to be published by this author.
2. R.B. Firestone, R.A. Warner, Wm. C. McHarris, and W.H. Kelly, Phys. Rev. C 17 (1978) 718.
3. M. Blann and F. Plasil, nuclear evaporation code ALICE adapted for the MSU Cyclotron Laboratory Sigma-7 computer by W. Bentley, and modified to use measured masses by R.C. Pardo.
4. J. Deslauriers, S.C. Gujrathi, and S.K. Mark, Z. Phys. A283 (1977) 33.

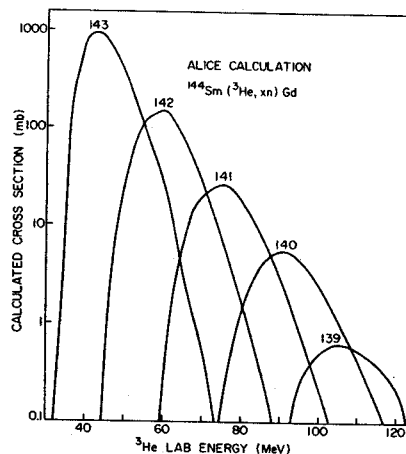


Fig. 1

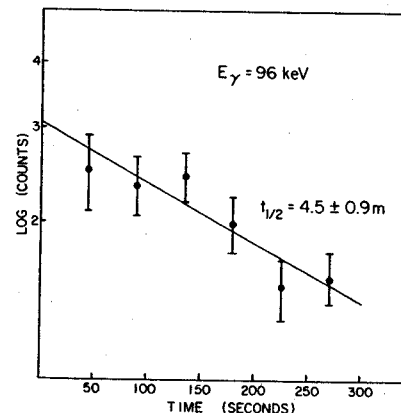


Fig. 2

The decay of  $^{145}\text{Gd}$  has aroused considerable interest in recent years because of the measurements at this laboratory of large anomalous EC/ $\beta^+$  decay branching ratios.<sup>1-3</sup> Recently Hornshøj, Nielson, and Rud<sup>4</sup> (hereafter HNR) challenged these measurements on the basis of previously unobserved feeding to states in  $^{145}\text{Eu}$  at high excitation as well as a very large error in the generally accepted electron capture  $Q_{\text{e}}$ -value of 5.3 MeV. We have obtained new data on  $^{145}\text{Gd}$  in an effort to answer these questions.

HNR make a number of strong claims which seem to be based largely on a  $\gamma$ -ray singles spectrum. First they maintain that they observe 16% of the total decay going through previously unreported  $\gamma$  rays with energies above 2.5 MeV. We had presented in an earlier Annual Report<sup>6</sup> a spectrum for  $^{145}\text{Gd}$  showing this high-lying feeding but had not pursued this question because the feeding appeared quite minor. Another  $\gamma$ -ray spectrum has since been obtained containing  $2 \times 10^9$  events after correction for long-lived contaminants and pile-up events. The spectrum above 4 MeV is shown in Fig. 1. Careful efficiency calibrations using numerous standard sources were performed in the exact geometry of the singles spectrum. The result of this analysis indicates that no more than 4% of the decay goes through new  $\gamma$  rays greater than 2.5 MeV. This alone is not sufficient to remove the anomalous  $\epsilon/\beta^+$  ratios; however, unobserved continuum  $\gamma$ -rays must yet be accounted for. A preliminary analysis of our data indicates <2% feeding to unobserved discrete transitions and a more sophisticated statistical analysis of the data is in progress. We do not understand the large intensity observed by HNR at this time.

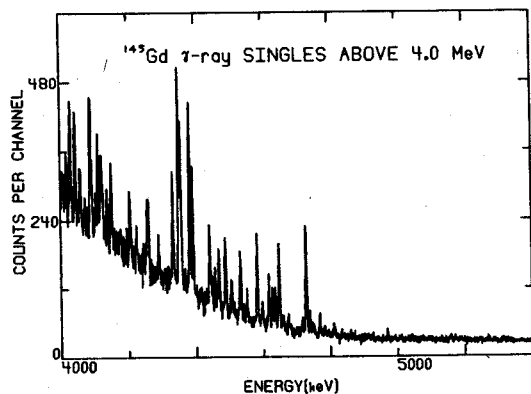


Fig. 1

A second conclusion drawn by HNR from their spectrum is that the available total decay energy for  $^{145}\text{Gd}$  is  $Q_{\text{e}} = 5.00 \pm 0.07$  MeV. They use the unorthodox technique of plotting the square root of the number of counts against the  $\gamma$  ray energy to

find the Q value. This assumes a constant decay strength and statistical feeding to levels in  $^{145}\text{Eu}$ . It is also presumed that the endpoint represents only K-capture decay. We find this method very objectionable because no effort is made to correct for Compton events which clearly dominate the spectrum; clustering of intensity is evident throughout the data, and at least some higher order capture decay must be considered. To emphasize these problems we have plotted our data in Fig. 2 in a similar manner to HNR. We have thirtyfold as many events as HNR analyzed and it is evident in our data that there is strong clustering. The best straight line through this data yields an endpoint at  $Q_{\text{e}} = 4.85$  MeV. If one assumes that this data represents essentially a "Compton-edge endpoint," approximately 240 keV must be added, yielding the real endpoint near 5.1 MeV. The literature value is  $Q_{\text{e}} = 5.3$  MeV so we decided to measure the decay energy in a more conventional form.

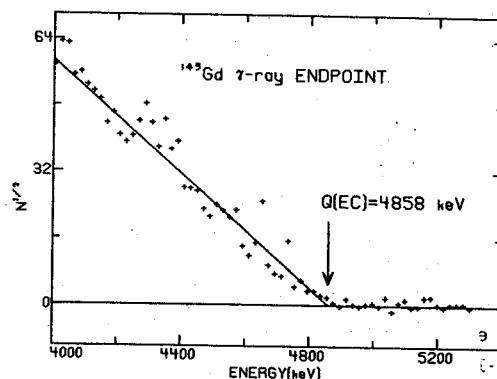


Fig. 2

Thin sources of  $^{145}\text{Gd}$  were produced by the  $^{144}\text{Sm}(\alpha, n)^{145}\text{Gd}$  reaction and deposited with a He-jet between a Ge(Li)  $\gamma$ -ray detector<sup>7</sup> and a 25.4 mm deep pilot B plastic scintillator.  $\beta$ - $\gamma$  coincidence spectra were recorded using conventional fast-slow coincidence techniques, and internal energy calibrations were performed using  $^{53}\text{Fe}$  and  $^{60}\text{Cu}$  sources produced by mixed targets. The data was analyzed by linearly stretching a strong gated  $\beta$  spectrum to obtain a stretch factor corresponding to the best fit. Stretch factors were obtained in this manner for both  $^{145}\text{Gd}$  and the standards using the strong transition from  $^{145}\text{Gd}$  to the 1758-keV state in  $^{145}\text{Eu}$  as the shape standard. Typical fits for the decay to the 1881-keV state in  $^{145}\text{Eu}$  and the 378 keV state in  $^{145}\text{Eu}$  are shown in Figs. 3 and 4. Fortuitously,

the stretch factors necessary were all very nearly equal to one, and only a small theoretical correction for the difference in  $Z$  between the standards and  $^{145}\text{Gd}$  was necessary. The resulting decay energy was determined as  $Q_{\epsilon} = 5.07 \pm 0.06$  MeV where a  $2\sigma$  statistical error is reported. This result is consistent with our interpretation of the  $\gamma$ -ray singles endpoint, and indeed lower than the literature value. We have therefore recalculated the  $\text{EC}/\beta^{+}$  ratios using the new value and present these results in Table I. Significantly anomalous  $\text{EC}/\beta^{+}$  ratios still remain, and in the last column of Table I we present the necessary missing EC feeding that remains to be found to reconcile the theory. At least 10% more decay must be uncovered to explain the anomalies and it does not appear that sufficient intensity remains yet to be placed. Recently a new  $^{145}\text{Gd}$   $\gamma$ - $\gamma$  coincidence experiment was performed in which  $1.3 \times 10^7$  events were recorded. This represents a large increase over our previous data. It is hoped that we can soon publish a much more complete decay scheme for  $^{145}\text{Gd}$ .

Table I

$^{145}\text{Gd}$   $\epsilon/\beta^{+}$  DECAY BRANCHING RATIOS

$^{145}\text{Eu}$ Level	$\epsilon/\beta^{+}$		Skew Ratio	"% Missing $\epsilon$ "
	Exp	Theory		
808	$18.0 \pm 8.0$	$0.56 \pm 0.01$	$32.0 \pm 15.0$	$2.6 \pm 0.4$
1042	$1.0 \pm 0.1$	$0.71 \pm 0.02$	$1.4 \pm 0.2$	$1.5 \pm 0.2$
1567	$37.0 \pm 18.0$	$1.26 \pm 0.05$	$29.0 \pm 15.0$	$1.0 \pm 0.2$
1600	$13.0 \pm 5.0$	$1.31 \pm 0.05$	$10.0 \pm 4.0$	$1.6 \pm 0.2$
1758	$1.87 \pm 0.09$	$1.62 \pm 0.06$	$1.15 \pm 0.10$	$3.2 \pm 0.9$
1762	$2.6 \pm 0.8$	$1.62 \pm 0.06$	$1.6 \pm 0.6$	$0.4 \pm 0.2$
1845	$43.0 \pm 25.0$	$1.82 \pm 0.07$	$24.0 \pm 15.0$	$0.6 \pm 0.2$
1881	$2.15 \pm 0.12$	$1.92 \pm 0.07$	$1.12 \pm 0.10$	$2.7 \pm 1.0$
2049	$4.2 \pm 1.0$	$2.47 \pm 0.12$	$1.7 \pm 0.5$	$0.4 \pm 0.2$
2114	$10.0 \pm 4.0$	$2.75 \pm 0.13$	$3.6 \pm 1.6$	$0.4 \pm 0.2$
2495	$4.8 \pm 0.5$	$5.44 \pm 0.34$	$0.9 \pm 0.2$	$-0.2 \pm 0.2$
2642	$8.1 \pm 0.9$	$7.55 \pm 0.58$	$1.1 \pm 0.2$	$0.1 \pm 0.2$

Net "missing"  $\epsilon$   $14.3 \pm 4.1\%$

1. R.B. Firestone, R.A. Warner, Wm. C. McHarris, and W.H. Kelly, Phys. Rev. Lett. 33 (1974) 30.
2. R.B. Firestone, R.A. Warner, Wm. C. McHarris, and W.H. Kelly, Phys. Rev. Lett. 35 (1975) 401.
3. R.B. Firestone, R.A. Warner, Wm. C. McHarris, and W.H. Kelly, Phys. Rev. Lett. 35 (1975) 713.
4. P. Hornshøj, H.L. Nielsen, and N. Rud, Phys. Rev. Lett. 39 (1977) 537.
5. T.W. Burrows, Nucl. Data Sheets 12 (1974) 203.
6. R.B. Firestone, R.A. Warner, Wm. C. McHarris, and W.H. Kelly, MSU Cyclotron Laboratory Annual Report 1974-1976, pp. 71-72.

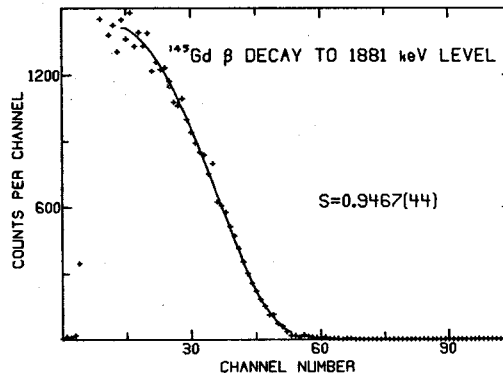


Fig. 3

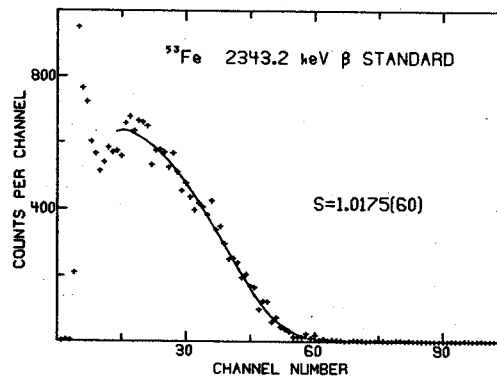


Fig. 4

The W and Hf region of deformed nuclei is one in which high-K multi-quasiparticle states abound. Much work has been done on  $^{174-178}\text{Hf}$  and  $^{178-182}\text{W}$  with fruitful results, and we report here preliminary results of our study of  $^{180}\text{W}$ . The  $^{180}\text{W}$  was produced by 48 MeV  $\alpha$ -particles on an enriched  $^{180}\text{Hf}$  target in the  $^{180}\text{Hf}(\alpha, 4n\gamma)^{180}\text{W}$  reaction. A fast timing experiment over a 350 ns time range showed a strongly populated delayed band, assumed to be built on the 5.2 msec,  $K^\pi=8^-$  isomer. Fig. 1 shows an  $(E_I - E_{I-1})/2I$  vs.  $2I^2$  plot of the presumed  $8^-$  band. A delayed coincidence experiment was performed to look at both the prompt decay from the isomer feeding the  $8^-$  band, and prompt feeding of the isomers. Four parameter data, including a beam pulse TAC in addition to the usual  $\gamma$ - $\gamma$  TAC and energy signals were acquired. The  $8^-$  band showed up clearly in the beam-off, prompt decay gates and showed that it was fed by an isomer at 3264 keV (Fig. 2). A beam pulsing experiment showed the half life of the isomer to be  $2.5 \pm 0.5$  sec. Delayed coincidence gates in the  $8^-$  band show additional transitions feeding the isomer, including lines at 92, 125, and 158 keV.

The 2.5  $\mu\text{sec}$ . isomer is probably a 4-quasiparticle,  $K^\pi=14^-$  isomer judging from the decay into the  $8^-$  band. The proton orbitals near the Fermi surface for  $\epsilon_2$  0.24,  $Z=74$  are  $9/2^-$  (514),  $5/2^+$  (402), and  $7/2^+$  (404), which when combined with the  $8^-$  two neutron  $9/2^+$  (624)  $\otimes$   $7/2^-$  (514) state gives the isomer possible spins of  $16^+$ ,  $15^-$ , or  $14^-$ . Since the isomer feeds the  $12^-$  level via an 813.4 keV transition, the  $14^-$  assignment is most probable.

The  $K^\pi=2^-$  octupole band, seen clearly to spin  $14^-$ , has also been observed at Livermore in the  $^{181}\text{Ta}(p, 2n\gamma)^{180}\text{W}$  reaction.<sup>1</sup> The  $2^-$  and probably  $3^-$  levels were also seen<sup>2,3</sup> in the decay of  $^{180}\text{Re}$ . Only the crossover transitions are seen in our data. The plot in Fig. 1 shows the odd spin members of the  $2^-$  band depressed in energy with respect to the even spin members, an effect attributed to mixing with the  $K^\pi=0^-$  octupole band.

Another band, the  $K=5^\pm$  or  $6^\pm$  is seen feeding into the  $K^\pi=2^-$  band with a half life of about 26 nsec. This third band may be the expected  $6^+$  two proton structure. Further analysis of our data may allow characterization of this band on the basis of multipolarity assignments or  $g_k$  values deduced from intraband branching ratios.

Further work is in progress to extend the level scheme to higher spins and place several additional lines.

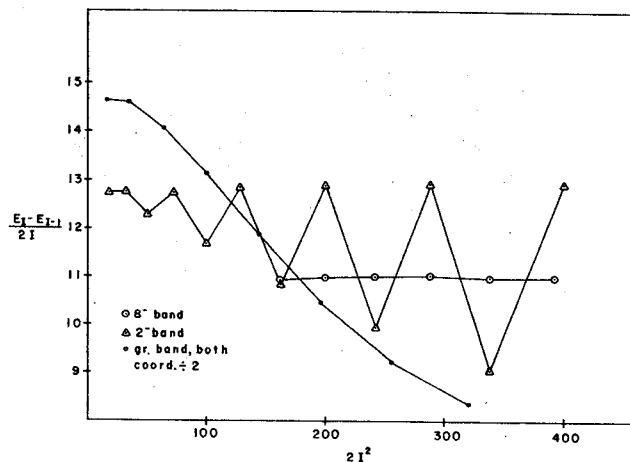


Fig. 1

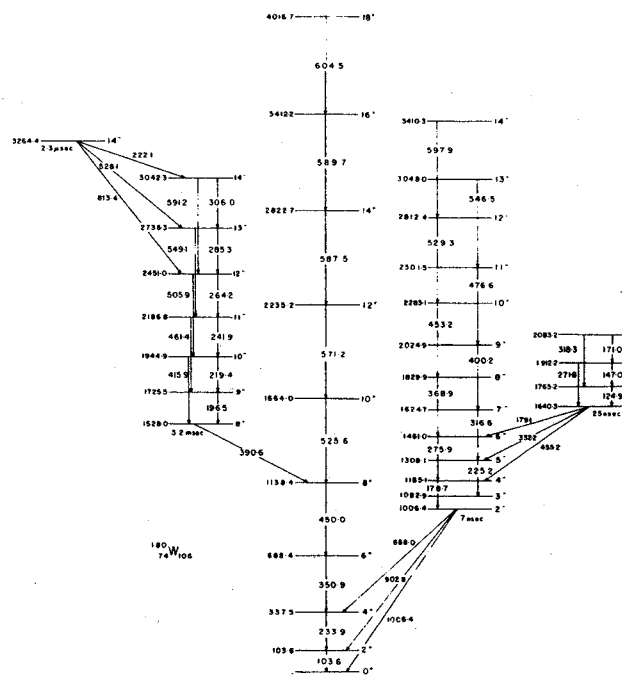


Fig. 2

\* Present address: Argonne National Laboratory, Argonne, IL.

\*\* Present address: Battelle N.W. Laboratory, Richland, WN.

1. L.G. Mann, J.B. Carlson, R.G. Lanier, G.L. Struble, and R.K. Sheline, preprint, Lawrence Livermore Laboratory, 1978.

2. K.J. Hoffstetter and P.J. Daly, Phys. Rev. **159** (1967) 1000.

3. P.F.A. Goudsmit, J. Konijn, and F.W.N. de Boer, Nucl. Phys. **A104** (1967) 497.



In an effort to understand the complex structure of the more neutron deficient odd-A platinum  $^{187}\text{Pt}$  and  $^{189}\text{Pt}$ , an extensive set of experiments was performed. The level schemes, though still incomplete, reveal several interesting features and differ in some respects from the spectra of  $^{191}\text{Pt}$  and  $^{193}\text{Pt}$ .<sup>1</sup> Investigation of  $^{189}\text{Pt}$  included prompt and delayed  $\gamma$ -ray singles,  $\gamma$ - $\gamma$ -t coincidence, excitation function and angular distribution determinations using the  $(\alpha,3n\gamma)$  reaction on an isotopically enriched  $^{188}\text{Os}$  (87%) target, and  $\gamma$ -ray singles measurements with the  $^{191}\text{Ir}(p,3n\gamma)$  reaction. In the study of  $^{187}\text{Pt}$  similar measurements were performed using the  $(\alpha,3n\gamma)$  reaction on  $^{186}\text{Os}$  (62%); complementary  $\gamma$ -ray singles data were obtained from the  $^{180}\text{Hf}(^{12}\text{C},5n\gamma)$  and  $^{188}\text{Os}(^3\text{He},4n\gamma)$  reactions.

On the basis of these experiments the level schemes shown in Figs. 1 and 2 were established. They contain extensive even parity  $\nu_{13/2}$  level families similar to those previously observed in  $^{191}\text{Pt}$  and  $^{193}\text{Pt}$ , viz. strongly populated favored decoupled bands with spacings resembling those of the even-even cores, and unfavored  $I+2$  sequences.<sup>1</sup> A discussion of the odd parity bands built on  $21/2^-$  states has been published.<sup>2</sup> These bands are thought to consist of an  $i_{13/2}$  neutron hole coupled to the  $5^-$ ,  $7^-$ , etc. states in the even Pt nuclei in analogy with similar bands found in neighboring odd-A Hg nuclei. This sequence may show a slightly different behavior in  $^{189}\text{Pt}$  as there is evidence both from our angular distribution data and from conversion electron measurements<sup>3</sup> indicating M1 for the strong 184-keV transition.

In  $^{189}\text{Pt}$  the  $11/2^+$  unfavored state is located only 11 keV above the  $13/2^+$  state. Comparison with the corresponding  $11/2^+$  levels in  $^{191,193}\text{Pt}$  shows that the energy of this level is decreasing with a decrease in mass number, until in  $^{187}\text{Pt}$  the  $11/2^+$  level drops below the  $13/2^+$  state. Support for this assignment comes from a recent delayed conversion electron spectrum<sup>3</sup> which revealed an intense transition of  $27\pm 3$  keV with preliminary coincidence results consistent with assignment as the  $13/2^+ \rightarrow 11/2^+$  transition.

Several odd parity bands accounting for a large fraction of the total transition strength are observed in  $^{189}\text{Pt}$ . The  $11/2^-$  level at 493 keV and the  $9/2^-$  level at 173 keV are populated in allowed  $\beta$ -decays<sup>4</sup> from  $^{189\text{m}}\text{Au}$  metastable state which is characterized as  $11/2^-$  (505) proton, thus associating the  $^{189}\text{Pt}$  levels with the  $h_{9/2}$  neutron orbital. In  $^{187}\text{Pt}$  there are three additional strong  $\gamma$ -ray cascades not shown in the level scheme. One of them, possibly of  $7/2^-$  (503) parentage deexcites by both cascade and cross-over transitions; a bandhead spin of  $7/2$  is consistent with excitation function data. The other two decay via  $\Delta I=2$  cascades and have probable band-head spins of  $7/2$  to  $11/2$ .

Low spin data for both  $^{189}\text{Pt}$  and especially  $^{187}\text{Pt}$  could be provided by radioactive decay studies, and may clarify some of the remaining problems in the level schemes of these nuclei.

- 
- \* Present address: University of Jyväskylä, Finland.  
 \*\* Present address: Queens University, Ontario.  
 + Present address: Argonne National Laboratory, Illinois.
1. S.K. Saha *et al.*, Phys. Rev. C 15 (1977) 94.
  2. M. Piiparinen *et al.*, Phys. Rev. Lett. 34 (1975) 1110.
  3. H. Backe *et al.*, Technische Hochschule Darmstadt, private communication.
  4. J. Jastrebski *et al.*, J. de Phys. 34 (1973) 755.

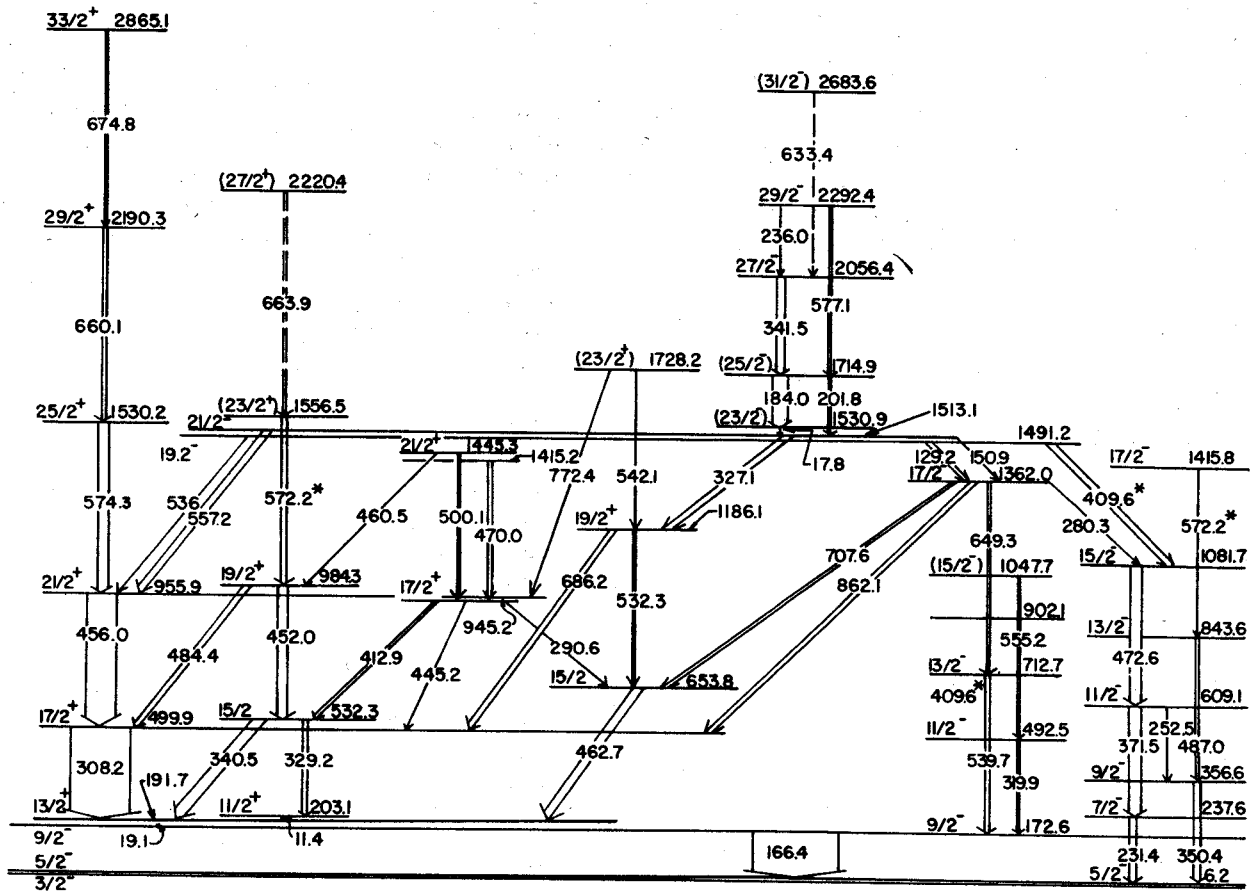


FIG. 1. The level structure of  $^{189}\text{Pt}$  deduced from  $(\alpha, 3n\gamma)$  and  $(p, 3n\gamma)$  studies.

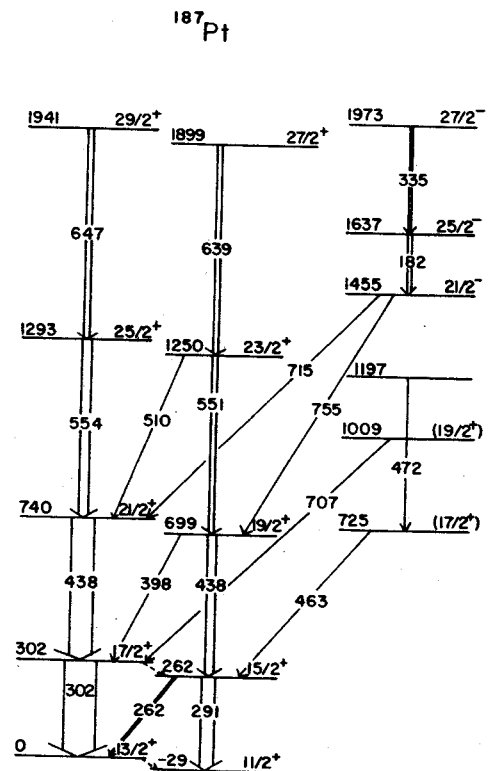


FIG. 2. A portion of the band structure of  $^{187}\text{Pt}$  observed in  $(\alpha, 3n\gamma)$ ,  $(^{12}\text{C}, 5n\gamma)$ , and  $(^3\text{He}, 4n\gamma)$  experiments.

# High-Spin Level Structure of $^{188}\text{Pt}$

P.J. Daly, C.L. Dors, H. Helppi,\* M. Piiparinen,\* S.K. Saha,\*\* F.M. Bernthal, and T.L. Khoo†

In the even-A platinum nuclei,  $A=186-194$ , acute backbending behavior at spin 10 in the even-parity yrast sequences has previously been reported.<sup>1,2</sup> This anomaly has been attributed to the intersection of the ground band by rotation-aligned  $\nu i_{13/2}^{-2}$  and  $\pi h_{11/2}^{-2}$  structures. Further investigation of  $^{188}\text{Pt}$  by ( $^{12}\text{C},4n\gamma$ ) studies and close examination of the extensive ( $\alpha,4n\gamma$ ) data has revealed several features which distinguish  $^{188}\text{Pt}$  from the higher mass even platinums.

The  $^{188}\text{Pt}$  level scheme is shown in Fig. 1. The ground band proceeds smoothly up to spin 12 with no sharp backbend, in contrast to the corresponding bands in  $^{190,192,194}\text{Pt}$ . Instead, in  $^{188}\text{Pt}$  the  $\gamma$ -band is perturbed by the intrusion of closely spaced  $10^+$  and  $12^+$  states which are at about the same excitation energy as the two-quasiparticle (qp) states in the other even platinums. The  $12^+$  state at 2810 keV and the  $10^+$  at 2663 keV are thus tentatively interpreted as rotation-aligned structures with configurations  $(\nu i_{12/2}^{-2})12^+$  and  $(\nu i_{13/2}^{-2})10^+$ , respectively. The  $12^+$  state has a decoupled band built on it having energy spacings resembling the ground band of the core. There is a third  $10^+$  state at 2702 keV. Recent experimental evidence from delayed conversion electron studies<sup>3</sup> indicates that a transition occurs between the two-qp  $12^+$  and the 2702-keV  $10^+$  also. The 102-keV transition, owing to its large conversion, is below our limits of detection. The  $10^+$  state suggested to lie at 2702 keV is tentatively assigned as the decoupled  $(\pi h_{11/2}^{-2})$  state.

Comparison of the three  $B(E2; 12^+ \rightarrow 10^+)$  values indicates that the  $12^+ \rightarrow 10^+_{\text{g.b.}}$  is down by a factor of almost 1000 from the others, while the  $B(E2)$  for the  $12^+$  to the  $10^+$  at 2663 is about a factor of two smaller than the  $B(E2; 2^+ \rightarrow 0^+)$ . Presumably, the upper two  $10^+$  states are mixed, so the  $12^+$  state deexcites rapidly to both of them, but the  $12^+ \rightarrow 10^+_{\text{g.b.}}$  proceeds only with great difficulty.

The rotation-aligned  $10^+$  state at 2663 keV depopulates to the  $8^+$  member of the  $\gamma$ -band. This mode of deexcitation would be favored by naive nuclear structure considerations, but it is not energetically favorable in the high mass platinums. It is only in the more deformed  $^{188}\text{Pt}$  that the  $8^+$  lies sufficiently low in energy to be strongly populated by the aligned  $10^+$  state.

One further feature of the  $^{188}\text{Pt}$  level structure is the occurrence of a negative parity band built on a  $5^-$  state. Similar semi-decoupled bands are observed in higher mass even-A platinum nuclei as well as in neighboring mercury nuclei.

- \* Present address: University of Jyväskylä, Finland.  
 \*\* Present address: Queens University, Ontario.  
 † Present address: Argonne National Laboratory, Illinois.
1. M. Piiparinen *et al.*, Phys. Rev. Lett. **34** (1975) 1110.
  2. L. Funke *et al.*, Phys. Lett. **5513** (1975) 436.
  3. H. Backe *et al.*, Technische Hochschule Darmstadt, private communication.

FIG. 1. The level scheme of  $^{188}\text{Pt}$  from ( $\alpha,4n\gamma$ ) and ( $^{12}\text{C},4n\gamma$ ) studies.

